Electronic Supplementary Information

for

Dioxygen Activation and Two Consecutive Oxidative Decarboxylations of Phenylpyruvate by Nonheme Iron(II) Complexes: Functional Models of Hydroxymandelate Synthase (HMS) and CloR

*Debobrata Sheet, Shrabanti Bhattacharya and Tapan Kanti Paine**

Department of Inorganic Chemistry, Indian Association for the Cultivation of Science,
2A & 2B Raja S. C. Mullick Road, Jadavpur, Kolkata-700032, India
E-mail: ictkp@iacs.res.in

EXPERIMENTAL SECTION

Materials and Physical Measurements

All chemicals and reagents were obtained from commercial sources and were used without further purification unless otherwise noted. Solvents were distilled and dried before use. Preparation, storage and handling of air-sensitive materials were carried out under an inert atmosphere in a glove box. Fourier transform infrared spectroscopy on KBr pellets was performed on a Shimadzu FT-IR 8400S instrument. Elemental analyses were performed on a Perkin Elmer 2400 series II CHN analyzer. Electro-spray ionization mass spectra were recorded with a Waters QTOF Micro YA263. ^{1}H NMR spectra were measured at room temperature using Bruker DPX-300 or 500 MHz NMR spectrometer. Solution electronic spectra (single and time-dependent) were measured on an Agilent 8453 diode array spectrophotometer. GC-MS measurements were carried out with a Perkin Elmer Clarus 600 using Elite 5 MS (30m x 0.25mm x 0.25µm) column with a maximum temperature of 300ºC. Labeling experiments were carried out with $^{18}O_2$ gas (99 atom %) or H_2O^{18} (98 atom %) purchased from Icon Services Inc., USA.

Synthesis of Ligands and Metal Complexes

The ligands $KTp^{Ph,Me}$ [1] and KTp^{Me2} [2] were synthesized according to the protocol reported in the literature.

[($Tp^{Ph,Me}$)Fe^{II}(PPH)] (1). A suspension of $FeCl_2$ (0.064 g, 0.5 mmol) and $KTp^{Ph,Me}$ (0.261 g, 0.5 mmol) in 10 mL dichloromethane was vigorously stirred for an hour. To the resulting mixture, methanolic solution (1 mL) of sodium phenylpyruvate (0.093 g, 0.5 mmol) was added. The resulting red solution was allowed to stir for 8 h and then solvent was removed to get a red solid residue. The residue was dissolved in dichloromethane (15 mL) and filtered. The filtrate was then dried to obtain a red solid. X-ray quality single-crystals were grown by vapor diffusion of diethyl ether into a dichloromethane solution of the complex. Yield: 0.28 g (80%). Anal. Cald. For $C_{39}H_{35}BFeN_6O_3$ (702.39 g/mol): C, 66.64; H, 5.02; N, 11.96. Found: C, 66.18; H, 5.19; N, 12.09%. ESI-MS (positive ion mode, CH_3CN): *m/z* (%) = 703.03 (5%), {[($Tp^{Ph,Me}$)Fe(PPH)]+H}$^+$; 725 (15%), {[($Tp^{Ph,Me}$)Fe(PPH)]+Na}$^+$; 539.12 (100%), [($Tp^{Ph,Me}$)Fe]$^+$. IR (cm^{-1}): 3382(br), 3058(w), 2925(w), 2856(w), 2545(w), 1695(s), 1681(s), 1585(w), 1544(s), 1479(w), 1436(m), 1413(m), 1367(w), 1301(w), 1186(s), 1174(s), 1066(m), 981(w), 763(s), 696(s), 638(w). UV-vis: λ_{max}, nm (ε, M^{-1} cm^{-1}): 422 (935), 552 (530). ^{1}H NMR (500 MHz, CD_3CN, 295 K): δ 58.14 (4-PzH), 27.34 (-CH_3 of $Tp^{Ph,Me}$), -13.51 (Ph of $Tp^{Ph,Me}$), 8.13 (Ph of $Tp^{Ph,Me}$), 7.32 (Ph of $Tp^{Ph,Me}$), -8.01 (-CH_2 of PPH) ppm.

[(Tp^{Me2})Fe^{II}(PPH)] (1a). To a solution of iron(II) chloride (0.127 g, 1 mmol) in methanol (10 mL) was added sodium phenylpyruvate (0.186 g, 1 mmol). To the red solution was added an acetonitrile solution

(5 mL) of KTp^{Me2} (0.336 g, 1 mmol) ligand. The resulting dark red solution was stirred at room temperature under nitrogen atmosphere for 10 h. The solvent was removed to dryness, re-dissolved with dichloromethane and filtered. The resulting filtrate was concentrated under vacuum and washed with hexane to isolate a red solid. Yield: 0.34 g (65%). ESI-MS (positive ion mode, CH_3CN): *m/z* (%) = 516.06 (100%), $\{[(Tp^{Me2})Fe(PPH)]\}^+$; 538.06 (5%), $\{[(Tp^{Me2})Fe(PPH)-H]+Na\}^+$; 554.03 (7%), $\{[(Tp^{Me2})Fe(PPH)-H]+K\}^+$; 353.08 (5%) $[(Tp^{Me2})Fe]^+$. IR (KBr, cm^{-1}): 3404(br), 2974(m), 2935(m), 2740(m), 2677(s), 2490(m), 1732(w), 1664(m), 1634(m), 1578(s), 1555(m), 1481(w), 1448(m), 1392(vs), 1114(m), 1028(m), 928(m), 800(m), 781(m), 745(w), 688(m). UV-vis in acetonitrile: λ_{max}, nm (ε, M^{-1} cm^{-1}): 413 (1350), 560 (720). ^1H NMR (300 MHz, CD_3CN, 295 K): δ 57.27 (4-PzH), 17.48 (5-Pz-CH_3 of Tp^{Me2}), -17.04 (3-Pz-CH_3 of Tp^{Me2}) ppm.

$[(Tp^{Ph,Me})Fe^{II}(PAA)]$ (2). A suspension of $FeCl_2$ (0.064 g, 0.5 mmol) and $KTp^{Ph,Me}$ (0.261 g, 0.5 mmol) in 10 mL dichloromethane was vigourously stirred for an hour. To the resulting mixture methanolic solution (1 mL) of sodium salt of phenylacetic acid (0.079 g, 0.5 mmol) was added. The resulting pale yellow solution was allowed to stir for 8 h and then dried under vacuum. The residue obtained was dissolved in dichloromethane (15 mL) and filtered. The filtrate was then dried and washed twice with 5 mL hexane to obtain a pale yellow solid. Yield: 0.23 g (68%). Anal. Cald. For $C_{38}H_{35}BFeN_6O_2$ (674.38 g/mol): C, 67.68; H, 5.23; N, 12.46. Found: C, 66.87; H, 5.31; N, 12.34%. ESI-MS (positive ion mode, CH_3CN): *m/z* (%) = 675.23 (25%), $\{[(Tp^{Ph,Me})Fe(PAA)]+H\}^+$; 539.02 (100%), $[(Tp^{Ph,Me})Fe]^+$. IR (cm^{-1}): 3411(br), 3261(w), 2677(w), 2491(w), 1600(s), 1566(m), 1546(s), 1433(s), 1392(m), 1413(m), 1301(w), 1176(m), 1068(m), 1033(w), 977(w), 765(s), 696(s). ^1H NMR (500 MHz, CD_3CN, 295 K): δ 58.11 (4-PzH), 25.96 (-CH_3 of $Tp^{Ph,Me}$), -10.22 (Ph of $Tp^{Ph,Me}$), 20.71 (Ph of $Tp^{Ph,Me}$), 16.64 (Ph of $Tp^{Ph,Me}$), 8.37 (PAA), 7.35 (PAA), 6.42 (PAA) ppm.

$[(Tp^{Ph,Me})Fe^{II}(mandelate)(CH_3OH)]$ (3). A suspension of $FeCl_2$ (0.064 g, 0.5 mmol) and $KTp^{Ph,Me}$ (0.261 g, 0.5 mmol) in 10 mL dichloromethane was vigorously stirred for an hour. To the resulting suspension, a methanolic solution (1 mL) of mandelic acid (0.076 g, 0.5 mmol) and triethyl amine (0.069 mL, 0.5 mmol) was added. The resulting colorless solution was allowed to stir for 8 h and then dried under vacuum. To the residue was added 10 mL dichloromethane and then filtered. The filtrate obtained was dried and washed twice with 5 mL hexane to obtain a white solid. Yield: 0.21 g (58%). Anal. Cald. For $C_{39}H_{39}BFeN_6O_4$ (722.42 g/mol): C, 64.84; H, 5.44; N, 11.63. Found: C, 64.37; H, 5.59; N, 11.83%. ESI-MS (positive ion mode, CH_3CN): *m/z* (%) = 539.34 (100%), $[(Tp^{Ph,Me})Fe]^+$. IR (cm^{-1}): 3433(br), 3062(w), 2929(w), 2474(w), 1700(w), 1695(m), 1681(s), 1569(m), 1504(m), 1469(m), 1411(m), 1348(w), 1267(w), 1296(w), 1195(m), 1169(m), 1116(w), 1091(s), 825(m), 761(vs), 692(vs), 644(w), 518(w). ^1H NMR (500 MHz, CD_3CN, 295 K): δ 55.64 (4-PzH), 21.74 (-CH_3 of $Tp^{Ph,Me}$), -21.51 (*o*-3-Ph of $Tp^{Ph,Me}$), -7.6 (CH-mandelate) ppm.

Reactivity with Dioxygen: A solution of the iron(II)-phenylpyruvate (0.02 mmol) in 10 mL dioxygen saturated CH_3CN was allowed to stir at room temperature. After the reaction, the solvent was removed under reduced pressure and the residue was treated with 10 mL 3M HCl. The organic products were extracted with diethyl ether and the organic phases were washed with brine solution. The combined organic part was dried over Na_2SO_4 and the solvent removed to dryness. The organic products were analyzed by ^{1}H-NMR spectroscopy. Quantification of the oxidized organic products were done by the addition of 2,4-di-*tert*-butylphenol (0.02 mmol) as an internal standard. Quantification of phenylacetic acid was done by comparing the peak area of the two benzylic protons (δ 3.67 ppm) with respect to one C-H proton of 2,4-di-*tert*-butylphenol (δ 6.58 ppm). The formation of benzoic acid was identified by the peak at (δ 8.11 ppm) corresponding to the *ortho* proton of benzoic acid and mandelic acid was judged by the peak at (δ 5.24 ppm) corresponding to the C-H proton. Benzaldehyde was analyzed and quantified by GC-MS using calibration curve obtained with authenticated compound.

NMR Data: Phenylacetic acid: Yield: 58%, *m/z* = 136.14, ^{1}H NMR (500 MHz, $CDCl_3$) δ 7.27-7.60 (m, 5H), 3.67 (s, 2H) ppm. **Benzoic acid:** Yield: 8%, *m/z* = 122.11, ^{1}H NMR (500 MHz, $CDCl_3$) δ 8.11 (d, 2H), 7.63 (t, 1H), 7.48 (t, 2H) ppm. **Benzaldehyde:** Yield: 33%, *m/z* = 106.12, ^{1}H NMR (500 MHz, $CDCl_3$) δ 10.03 (s, 1H), 7.53 (t, 2H), 7.63 (t, 1H), 7.88 (d, 2H) ppm.

Interception Studies with Various Substrates (9,10-Dihydroanthracene, Thioanisole, Dibenzothiophene and Fluorene): The iron(II) complex (0.02 mmol) was dissolved in 10 mL dry acetonitrile. To the solution 10 eqv (0.2 mmol) of external substrates (9,10-dihydroanthracene, thioanisole, fluorene and dibenzothiophene) was added. The solution was then saturated with dioxygen by purging dioxygen for 5 min and the reaction was allowed to continue for 90 min at room temperature under dioxygen atmosphere. The reaction solution was then dried by rotary evaporator and the residue was treated with 3.0 M HCl solution (10 mL). The organic products were extracted with diethyl ether (3x15 mL) and washed with brine solution. The combined organic phase was then dried over Na_2SO_4 and the solvent was removed under high vacuum. The organic products were then analyzed by ^{1}H NMR spectroscopy or by GC-MS using calibration curve obtained with authenticated compound.

Formation of thioanisole oxide from thioanisole was monitored by the appearance of peak at (δ 2.76 ppm) corresponding to the methyl protons. Quantification of thioanisole oxide was done by comparing the peak area of the three protons $-CH_3$ (δ 2.76 ppm) with one proton (δ 6.58 ppm) of 2,4-di-*tert*-butylphenol used as internal standard. The formation of anthracene and fluorenone from 9,10-dihydroanthracene and fluorene, respectively, were analyzed by GC-MS and quantified using calibration curves obtained with authenticated compounds.

Interception Studies with Dimethyl Sulfoxide: Complex **1** (0.02 mmol) was dissolved in dry acetonitrile (10 mL). To the solution was added 10 eqv of dimethyl sulfoxide (0.2 mmol). Dry dioxygen gas was bubbled through the solution for 5 min and the solution was stirred at room temperature under

oxygen atmosphere for 90 min. The solvent was then removed from the reaction mixture and distilled benzene was added. A slight excess of sodium dithionite (0.04 mmol) was then added to the benzene solution followed by addition of D_2O (1 mL) and the resulting solution was stirred for 15 min. To the solution was added 1,10-phenanthroline monohydrate (0.06 mmol) and stirred for an additional 30 min. The D_2O layer was then collected and analyzed by ^1H NMR spectroscopy. ^1H NMR data of dimethyl sulfone from dimethyl sufoxide (500 MHz, D_2O, 295 K): δ 3.17 (s, 6H) ppm.

Interception Studies with Various Alkenes (1-Octene, Cyclooctene and Cyclohexene): The iron(II)-phenylpyruvate complex (0.02 mmol) was dissolved in 10 mL dry acetonitrile and 10 eqv (0.2 mmol) of external reagent was added. Dioxygen was purged through the solution for 5 min and the reaction solution was allowed to stir at room temperature for 90 min. The organic solvents were removed under reduced pressure and the residue was treated with 3.0 M HCl solution (10 mL). The organic products were extracted with diethyl ether (3x15 mL) and washed with brine solution. The combined organic phase was then dried over Na_2SO_4 and the solvent was removed under vacuum. The organic products were then analyzed by ^1H NMR spectroscopy or by GC-mass spectrometry.

NMR Data of the Oxidized Products: Octane-1,2-diol: ^1H NMR (500 MHz, $CDCl_3$), δ 3.80-3.63 (m, 2H), 3.49 (m, 1H), 1.44-1.40 (m, 2H), 1.30-1.24 (m, 6H), 0.92-0.86 (m, 3H) ppm. ***cis*-Cyclooctane-1,2-diol:** ^1H NMR (500 MHz, $CDCl_3$), δ 3.94 (d, 2H), 1.93-1.86 (m, 2H), 1.70-1.63 (m, 4H), 1.55-1.49 (m, 6H) ppm**.** ***cis*-Cyclohexane-1,2-diol:** ^1H NMR (500 MHz, $CDCl_3$), δ 3.77-3.82 (m, 2H) 3.58 (br s, 2H), 1.73-1.82 (m, 2H), 1.51-1.64 (m, 4H), 1.27-1.35 ppm (m, 2H) ppm.

X-ray Crystallographic Data Collection and Refinement of the Structure of 1: X-ray single-crystal data for **1** were collected at 120 K using Mo K_α (λ = 0.7107 Å) radiation on a SMART-APEX diffractometer equipped with CCD area detector. Data collection, data reduction, structure solution and refinement were carried out using the software package of APEX II.[3] The structure was solved by direct method and subsequent Fourier analyses and refined by the full-matrix least-squares method based on F^2 with all observed reflections.[4] The non-hydrogen atoms were treated anisotropically.

Crystal data of **1**: MF = $C_{39}H_{35}BFeN_6O_3$, Mr = 702.39, Orthorhombic, space group Pbca, a = 11.861(2), b = 22.463(4), c = 25.580(5) Å, α = 90.00°, β = 90.00°, γ = 90.00°, V = 6815(2) Å^3, Z = 8, ρ = 1.369 mg m^{-3}, μMo-K_α = 0.491 mm^{-1}, F(000) = 2928, GOF = 1.187, A total of 45556 reflections were collected in the range 1.59≤ θ ≤ 19.86, 3118 of which were unique (R_{int} = 0.2167). R_1(*w*R*2*) = 0.0458 (0.1205) for 462 parameters and 2004 reflections (I > 2σ(I)). CCDC 1013639 contains the supplementary crystallographic data for this paper. The data can be obtained free of charge from the Cambridge Crystallographic Data Centre via www.ccdc.cam.ac.uk/data_request/cif.

Table S1 Selected bond distances (Å) and angles (°) of complex **1**.

Fe(1) – N(2)	2.184(7)	Fe(1) – N(3)	2.082(7)
Fe(1) – N(5)	2.076(7)	Fe(1) – O(1)	1.978(6)
Fe(1) – O(2)	2.258(6)	C(31) – O(1)	1.275(11)
C(31) – O(3)	1.226(10)	C(32) – O(2)	1.214(9)
C(32) – C(33)	1.502(12)	C(32) – C(31)	1.555(12)
C(33) – C(34)	1.494(12)	N(5) – Fe(1) – N(3)	93.6(3)
N(5) – Fe(1) – N(2)	86.2(3)	N(5) – Fe(1) – O(2)	88.0(2)
N(5) – Fe(1) – O(1)	135.2(3)	N(2) – Fe(1) – N(3)	91.5(3)
N(2) – Fe(1) – O(2)	174.3(2)	N(2) – Fe(1) – O(1)	106.6(3)
N(3) – Fe(1) – O(1)	127.7(3)	N(3) – Fe(1) – O(2)	89.1(2)
O(1) – Fe(1) – O(2)	77.4(2)	O(2) – C(32) – C(31)	117.1(8)
O(1) – C(31) – C(32)	115.1(8)	O(3) – C(31) – O(1)	127.1(9)
O(3) – C(31) – C(32)	117.8(9)	C(32)–C(33)–C(34)	114.9(7)
O(2) – C(32) – C(33)	123.1(8)	C(31) – C(32)–C(33)	119.8(9)

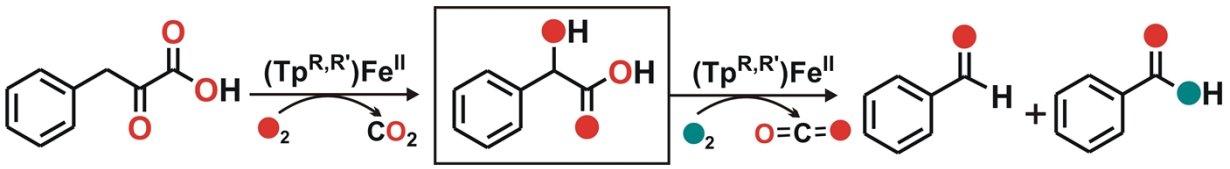

Scheme S1 Formation of benzoic acid from phenylpyruvic acid via mandelic acid in the reaction of the complexes (**1** and **1a**) with O_2.

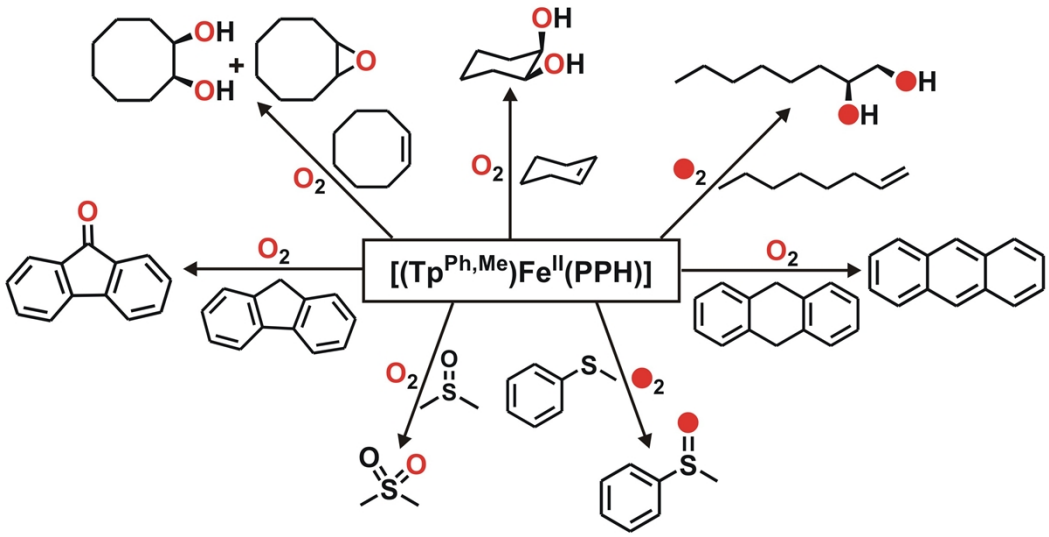

Scheme S2 Interception of the iron-oxygen oxidant formed in the oxidation of **1** with O_2.

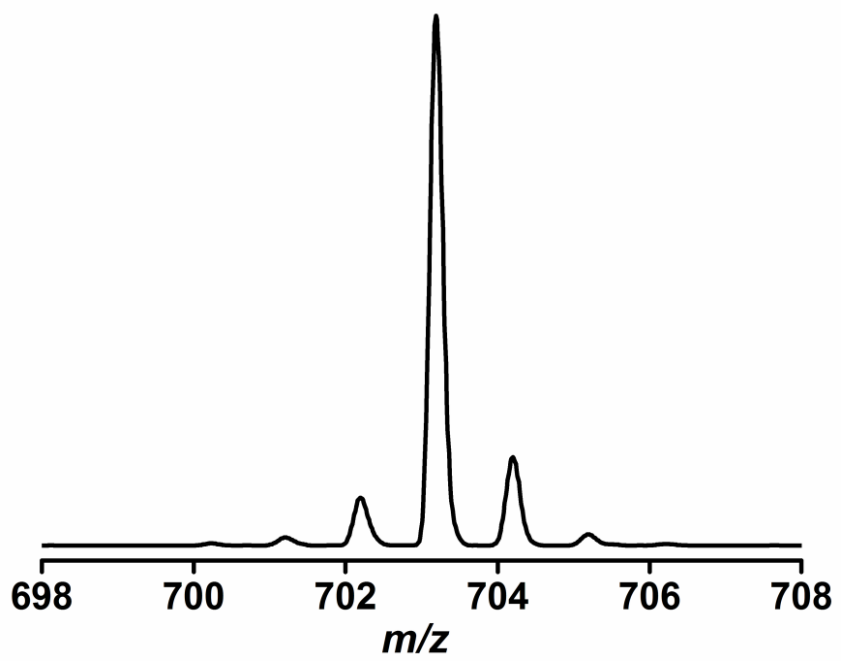

Fig. S1 ESI-mass spectrum (positive ion mode, acetonitrile) of [($Tp^{Ph,Me}$)Fe^{II}(PPH)] (**1**).

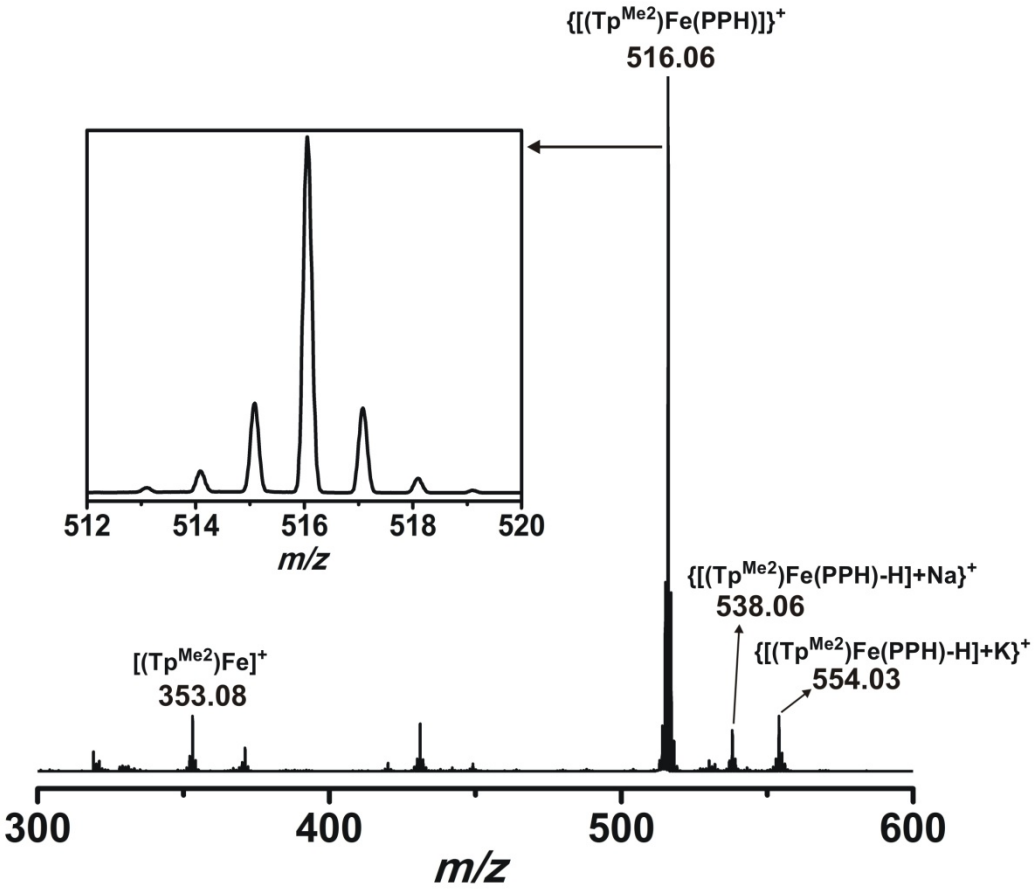

Fig. S2 ESI-mass spectrum (positive ion mode, acetonitrile) of [(Tp^{Me2})Fe^{II}(PPH)] (**1a**).

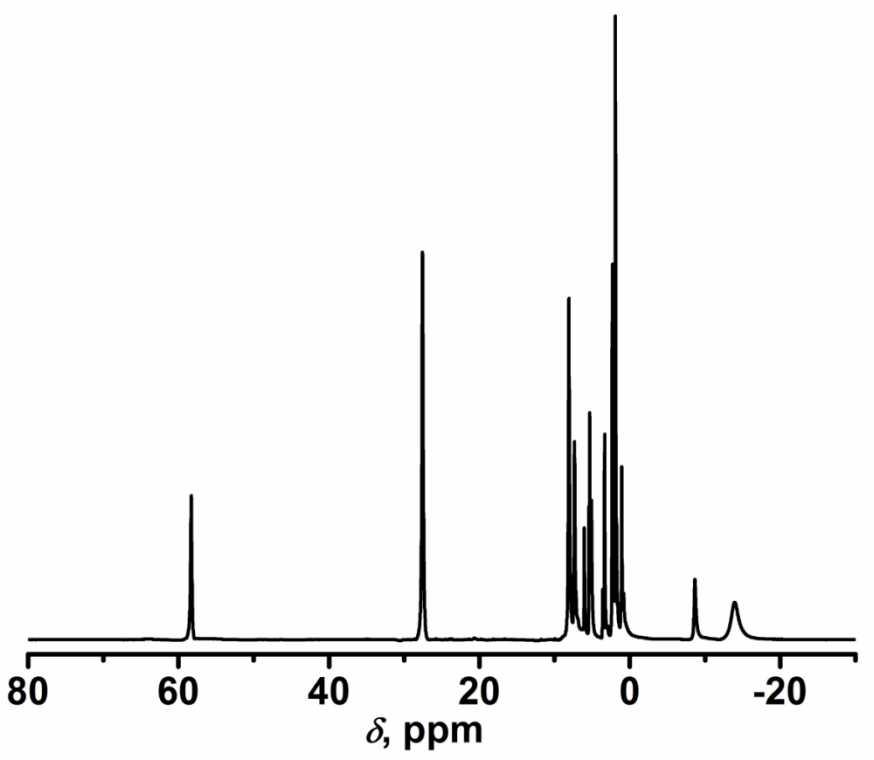

Fig. S3 ^{1}H NMR spectrum (500 MHz, CD_3CN, 295 K) of [($Tp^{Ph,Me}$)Fe^{II}(PPH)] (**1**).

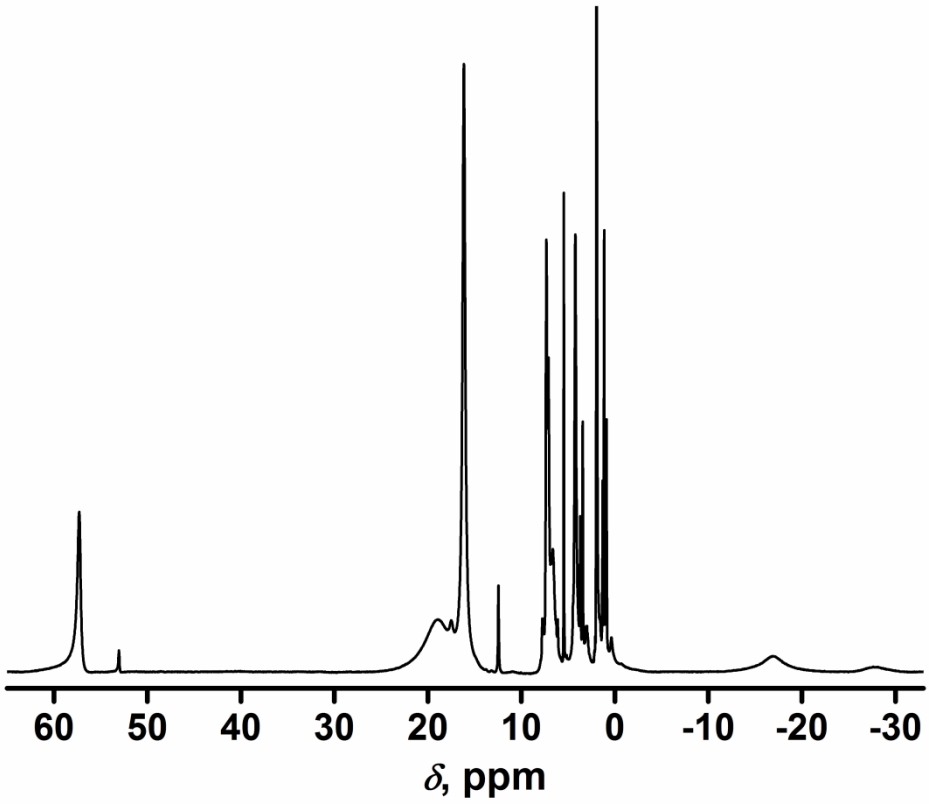

Fig. S4 ^{1}H NMR spectrum (300 MHz, CD_3CN, 295 K) of [(Tp^{Me2})Fe^{II}(PPH)] (**1a**).

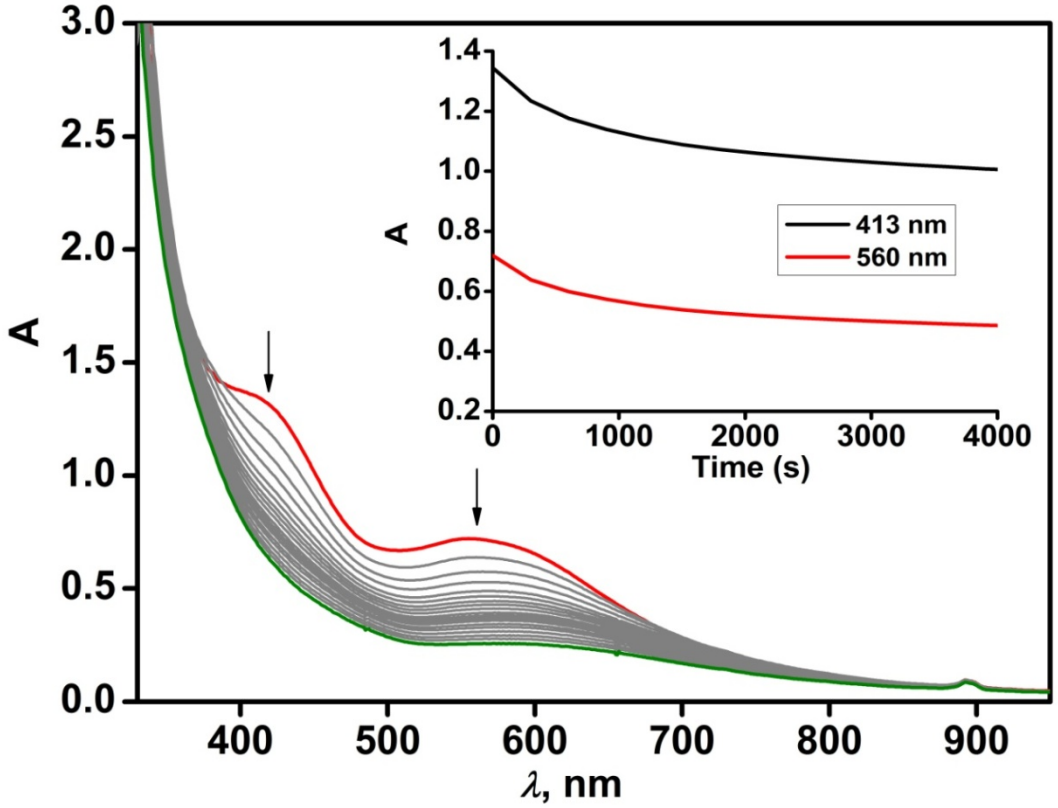

Fig. S5 Optical spectral changes during the reaction of **1a** (1 mM) with dioxygen in acetonitrile at 295 K.

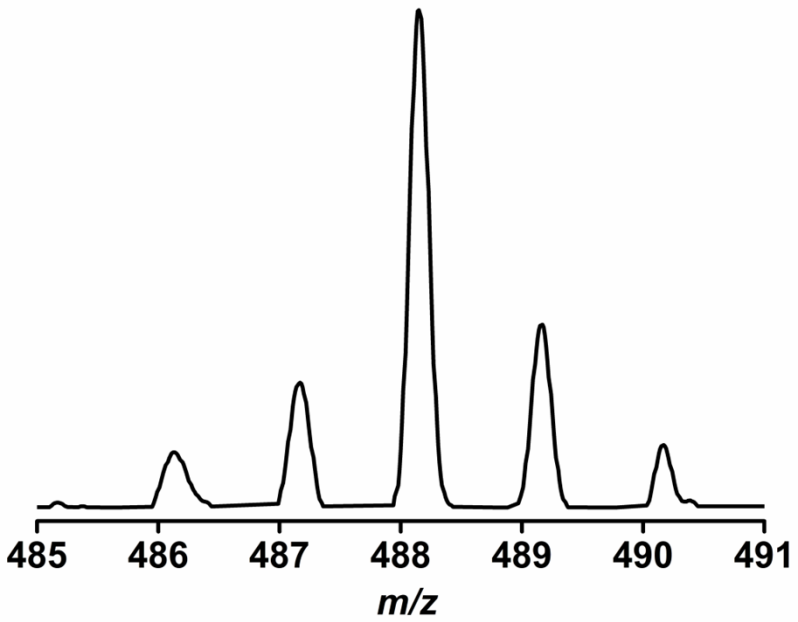

Fig. S6 ESI-mass spectrum (positive ion mode, acetonitrile) of the oxidized solution after the reaction of **1a** with O_2.

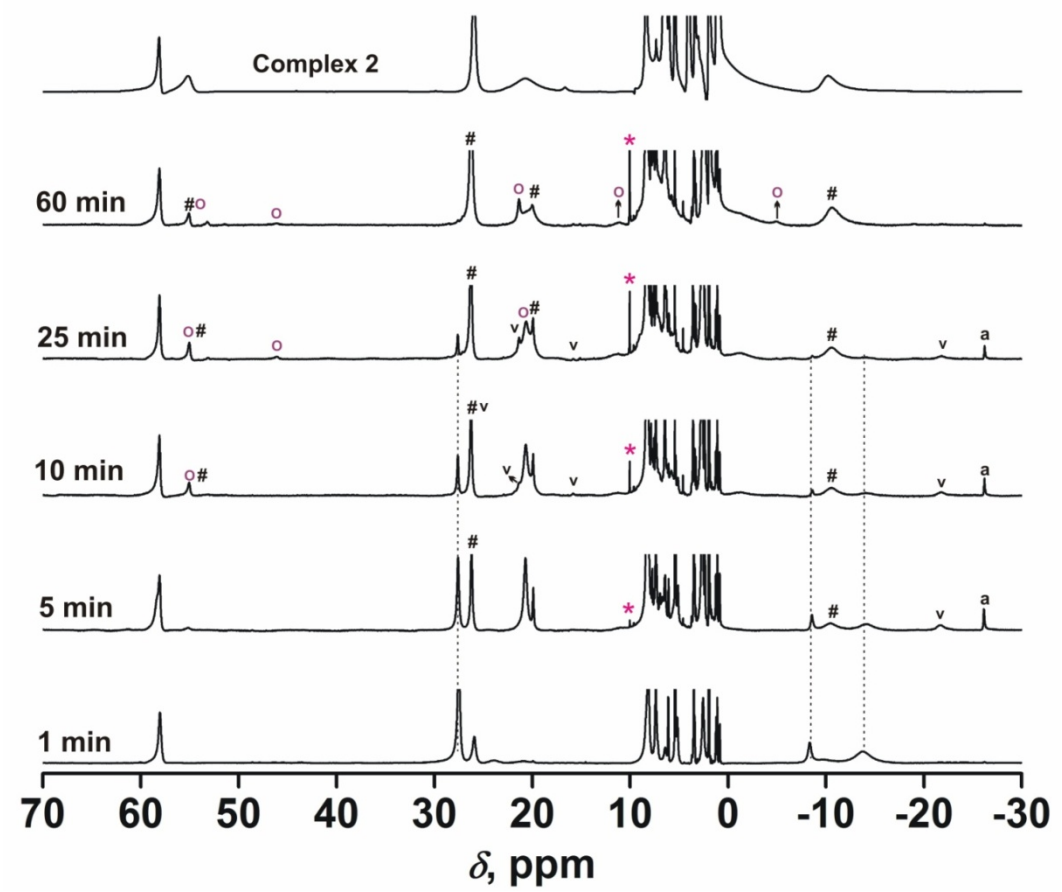

Fig. S7 Time-dependent ^{1}H NMR spectra (500 MHz, CD_3CN, 295 K) during the reaction of **1** with dioxygen. The vertical dotted lines indicate the decrease in intensity of the peaks associated with iron(II)-phenylpyruvate complex. Peak assigned with hash (#) indicates the formation of iron(II)-phenylacetate complex and the peaks derived from iron(II)-benzoate complex is marked as (o). Peaks assigned with (v) are derived from in situ formed iron(II)-mandelate complex Peaks assigned with asterisk (*) is from benzaldehyde. The peak marked with (a) likely arise from some unidentified intermediate species formed during the course of the reaction. Top: ^{1}H NMR spectrum (500 MHz, CD_3CN, 295 K) of complex **2**.

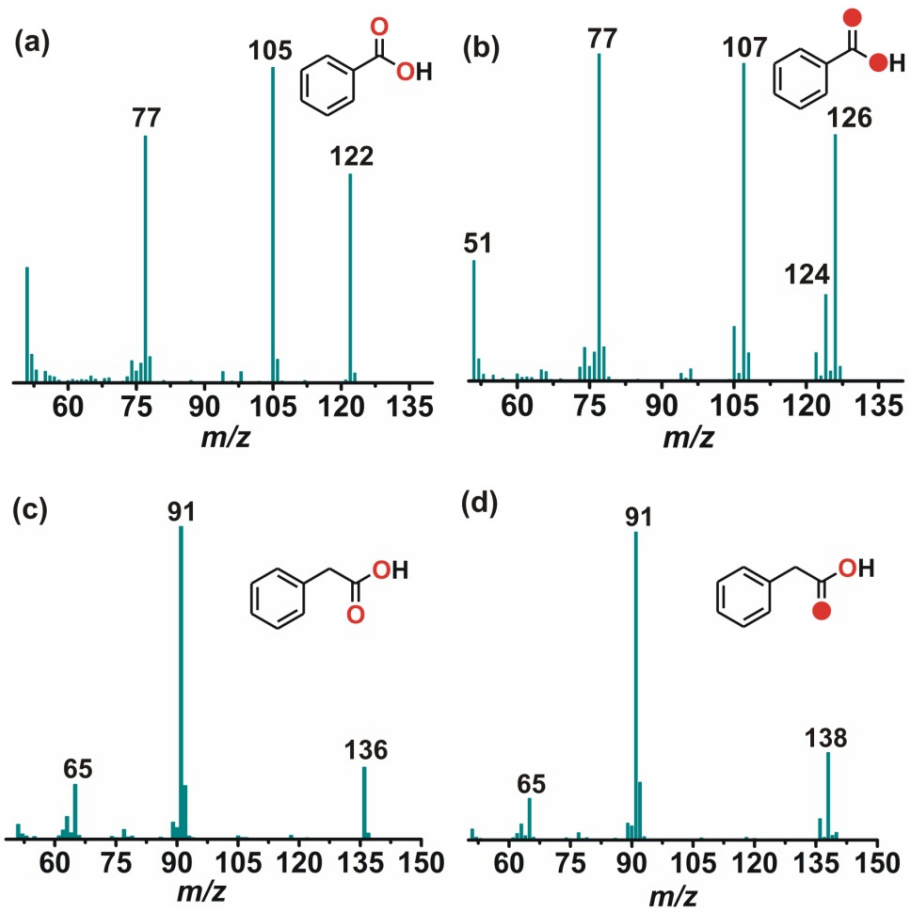

Fig. S8 GC-mass spectra of benzoic acid and phenylacetic acid formed in the reaction of **1** with $^{16}O_2$ (a and c) and with $^{18}O_2$ (b and d).

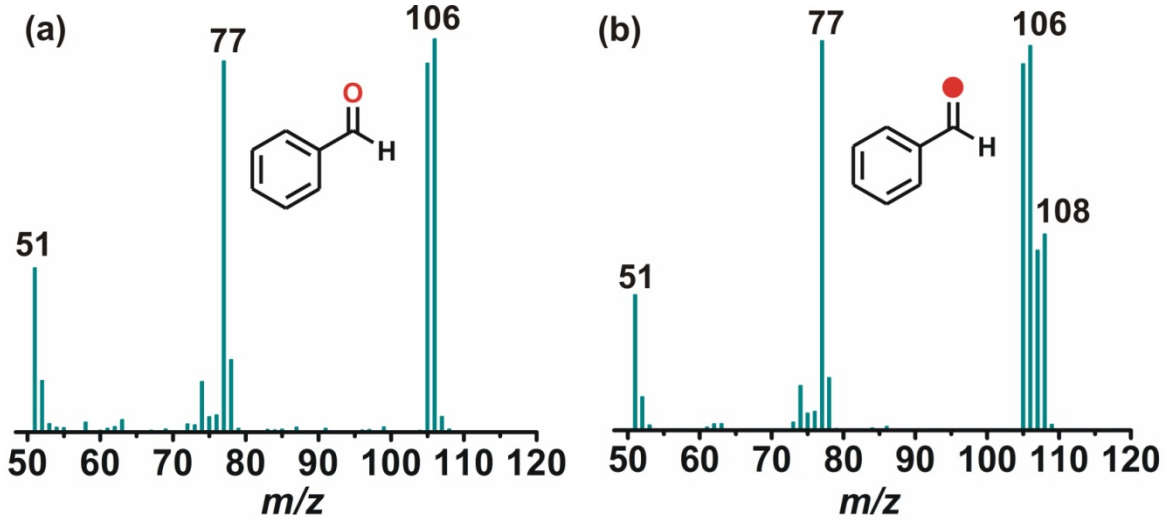

Fig. S9 GC-mass spectra of benzaldehyde formed in the reaction of **1** with (a) $^{16}O_2$ and with (b) $^{18}O_2$.

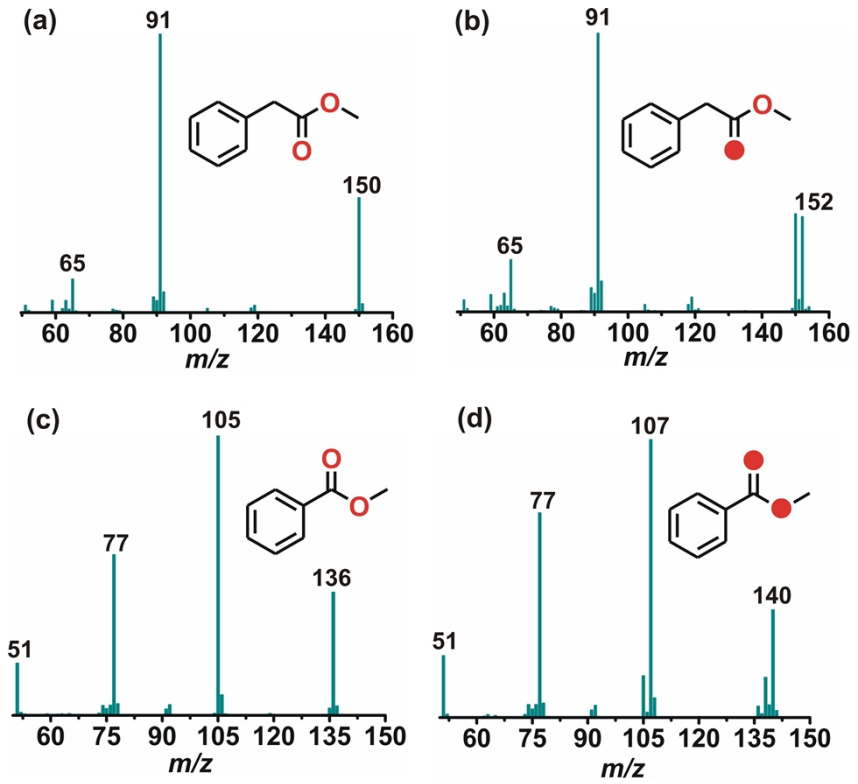

Fig. S10 GC-mass spectra of methyl esters of phenylacetic acid and benzoic acid. The acids are formed in the reaction of **1** with $^{16}O_2$ (a and c) and with $^{18}O_2$ (b and d).

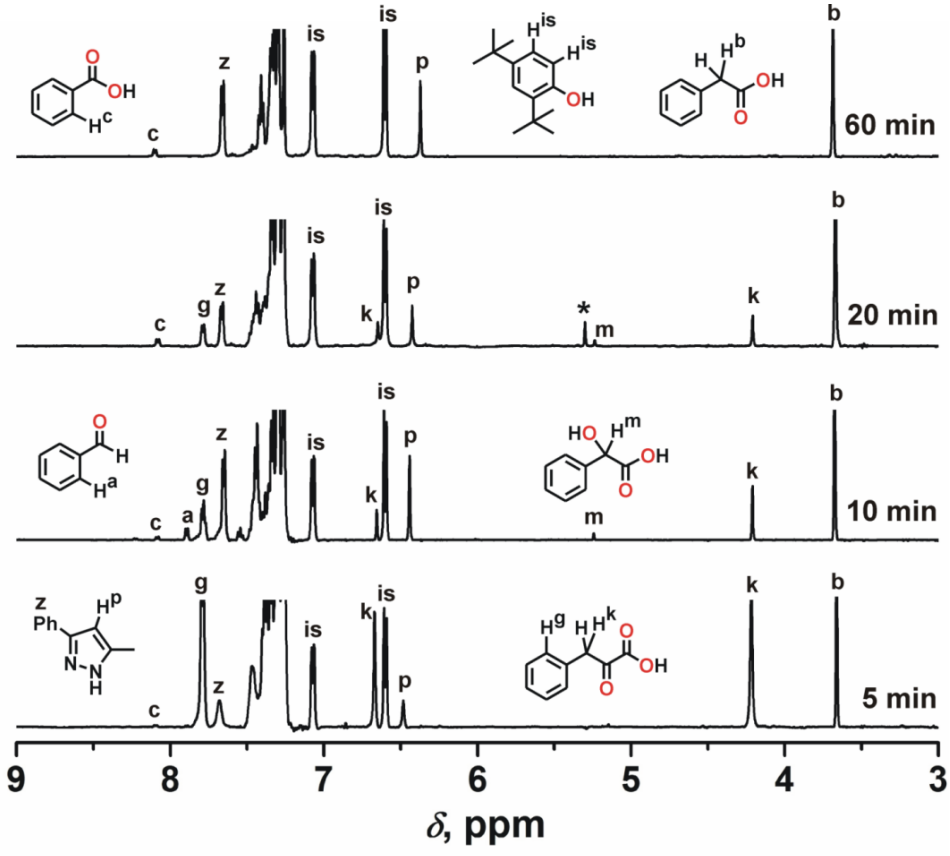

Fig. S11 Time-dependent ^{1}H NMR spectra (500 MHz in $CDCl_3$ at 298 K) of organic products formed in the reaction of **1** with dioxygen. Peak assigned with asterisk (*) is from residual solvent.

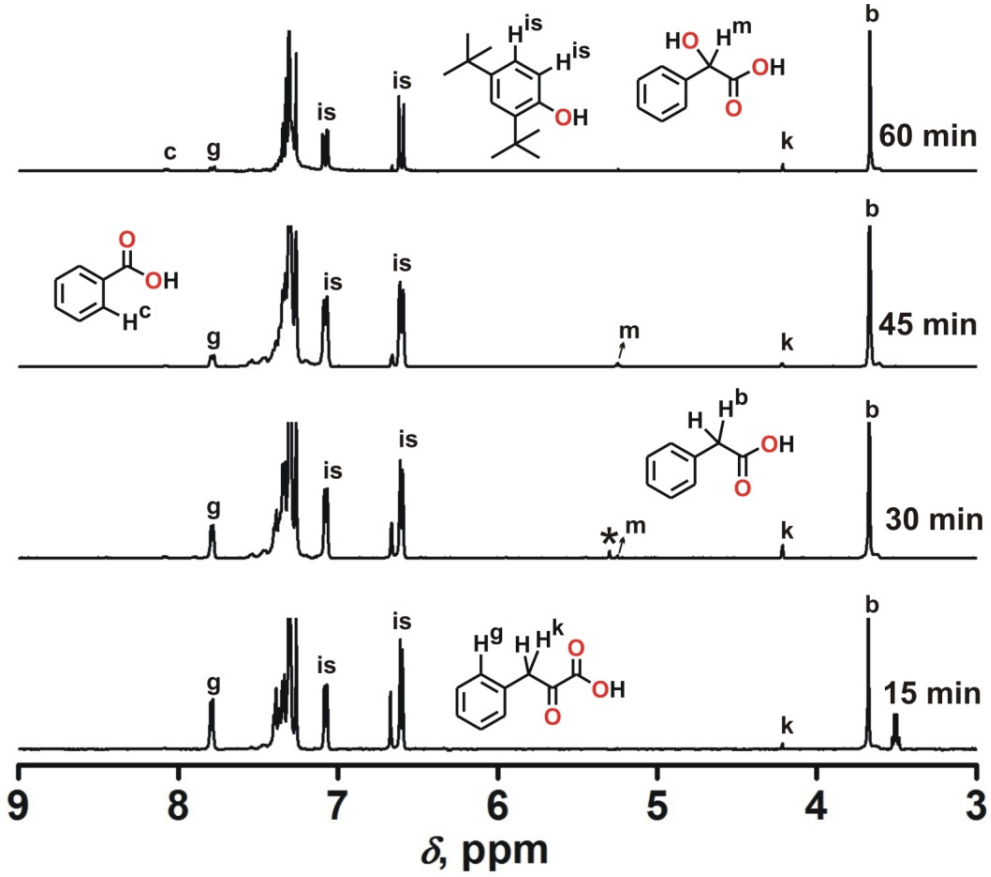

Fig. S12 Time-dependent ^{1}H NMR spectra (500 MHz in $CDCl_3$ at 298 K) of organic products formed in the reaction of **1a** with dioxygen. Peak assigned with asterisk (*) is from residual solvent.

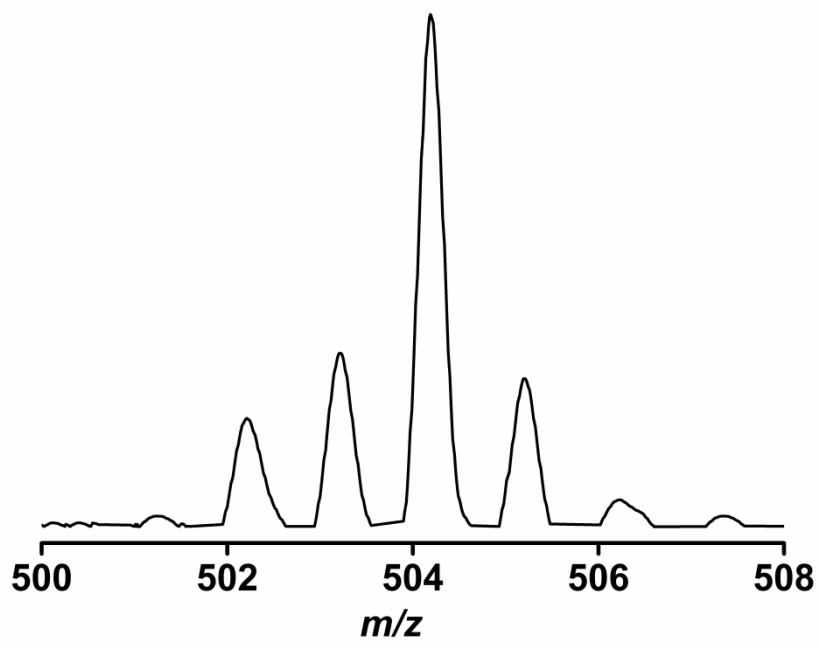

Fig. S13 ESI-mass spectrum (positive ion mode, acetonitrile) of the oxidized solution after the reaction of **1a** with O_2.

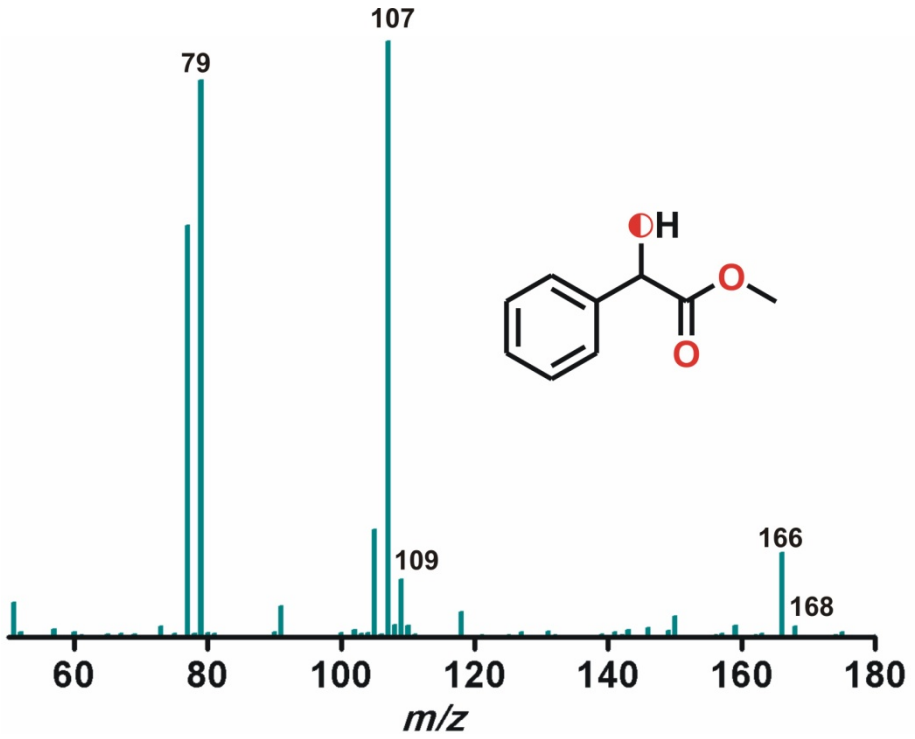

Fig. S14 GC-mass spectrum (positive ion mode, acetonitrile) of the methyl ester of mandelic acid. Mandelic acid is formed in the reaction of **1** with O_2 in the presence of H_2O^{18}.

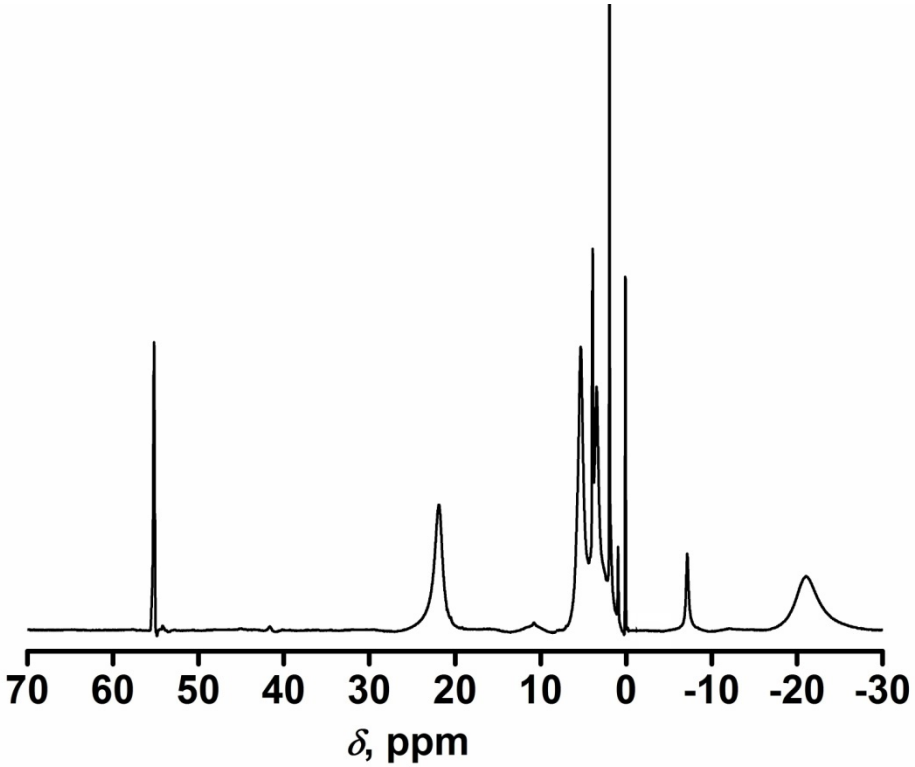

Fig. S15 ^{1}H NMR spectrum (500 MHz, CD_3CN, 295 K) of [($Tp^{Ph,Me}$)Fe^{II}(mandelate)(MeOH)] (**3**).

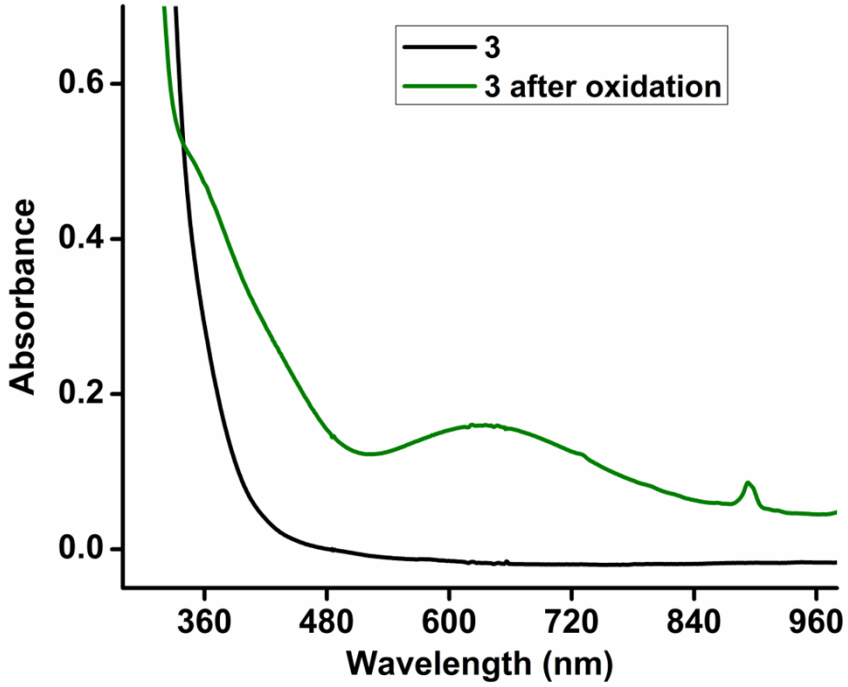

Fig. S16 Optical spectra of **3** (0.5 mM in acetonitrile) (black line) and after reaction with dioxygen (green line) at 298 K.

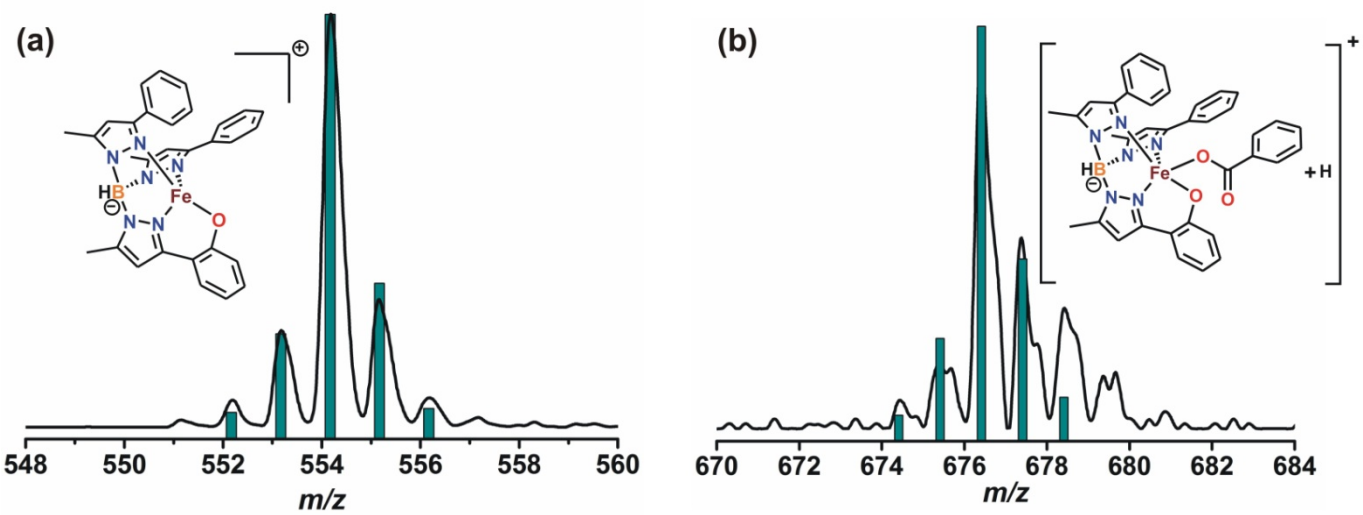

Fig. S17 ESI-mass spectra (positive ion mode, acetonitrile) of the final oxidized solution of **3** with the isotope distribution patterns calculated for $[(Tp^{Ph,\ Me*})Fe]^+$, and $\{[(Tp^{Ph,\ Me*})Fe(OBz)] + H\}^+$, where $Tp^{Ph,\ Me*}$ is a modified form of the ligand in which one of the ortho carbon of a 3-Ph ring gets hydroxylated and OBz is benzoate.

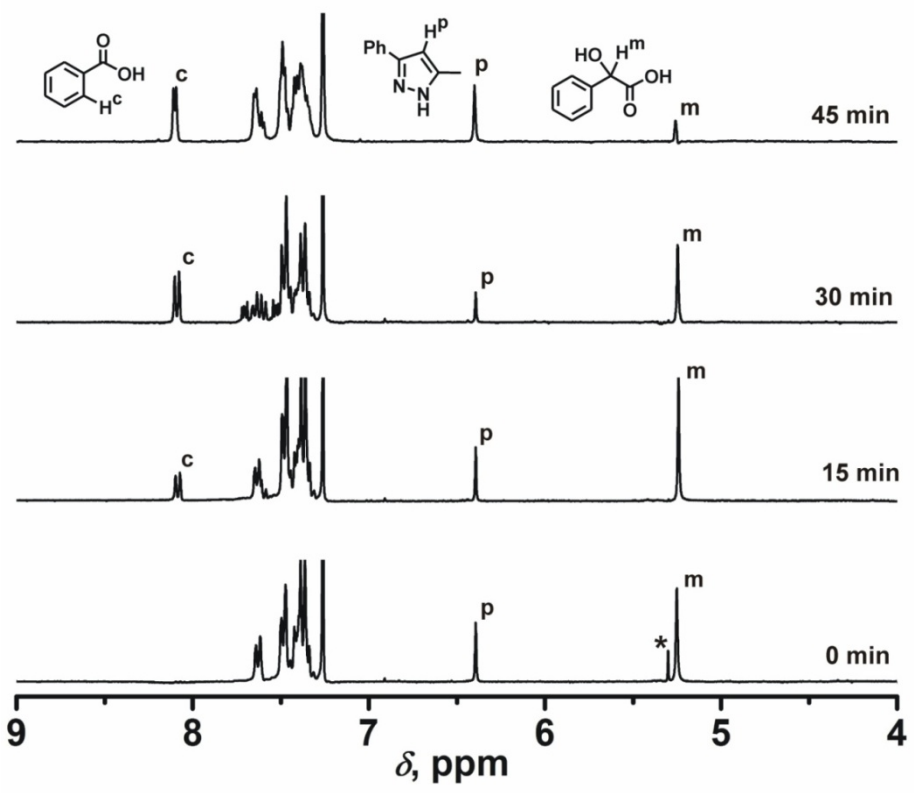

Fig. S18 ^{1}H NMR spectrum (500 MHz in $CDCl_3$ at 298 K) of the organic products derived in the reaction of **3** with dioxygen. Benzaldehyde and benzyl alcohol were quantified by GC. Peak assigned with asterisk (*) is from residual solvent.

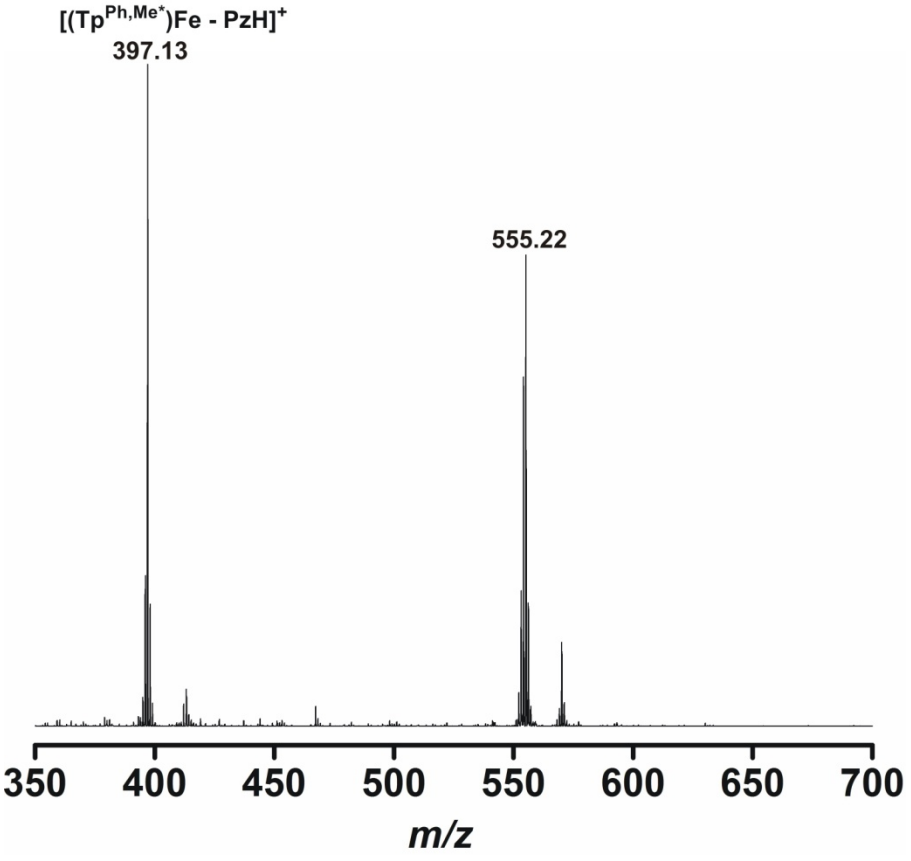

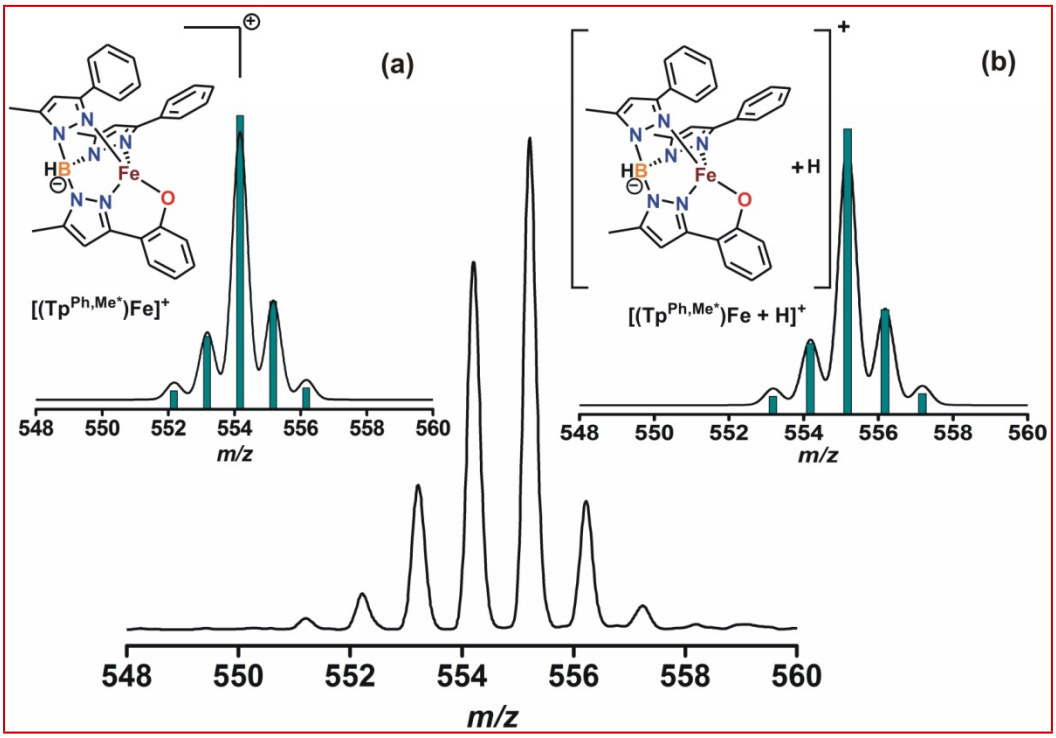

Fig. S19. Top: ESI-mass spectrum (positive ion mode) of the oxidized solution of **1** after reaction with O_2 for 2 h. Botton: Isotope distribution pattern of the peak at 555.22, Inset: (a) Computer simulated spectra of $[(Tp^{Ph,Me*})Fe]^+$ and (b) Computer simulated spectra of $\{[(Tp^{Ph,Me*})Fe]+H\}^+$ where $Tp^{Ph,Me*}$ is a modified form of the ligand in which one of the ortho carbon of a 3-Ph ring gets hydroxylated.

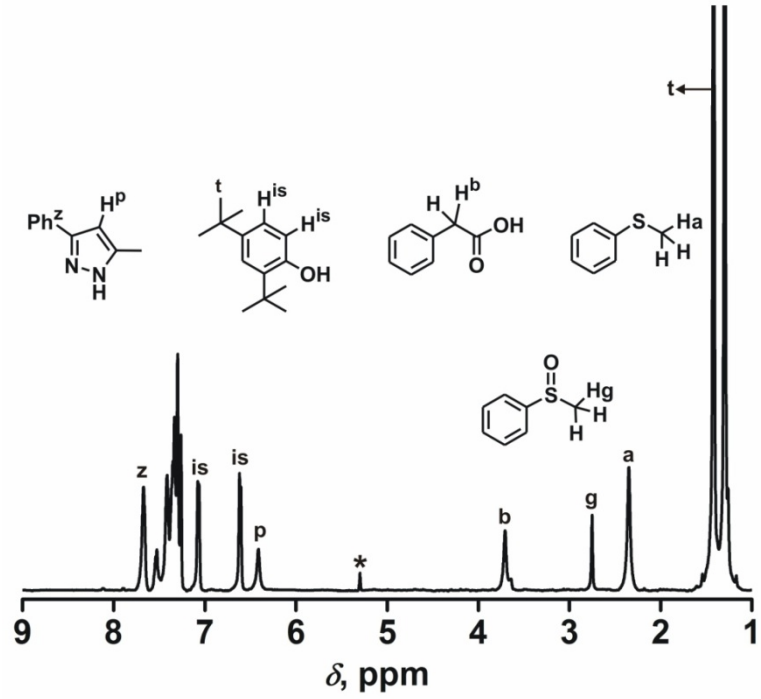

Fig. S20 ^1H NMR spectrum (500 MHz, $CDCl_3$, 295 K) of thioanisole-derived product after the reaction of **1** with O_2 in the presence of 10 eqv of thioanisole in acetonitrile. Peak assigned with asterisk (*) is from residual solvent.

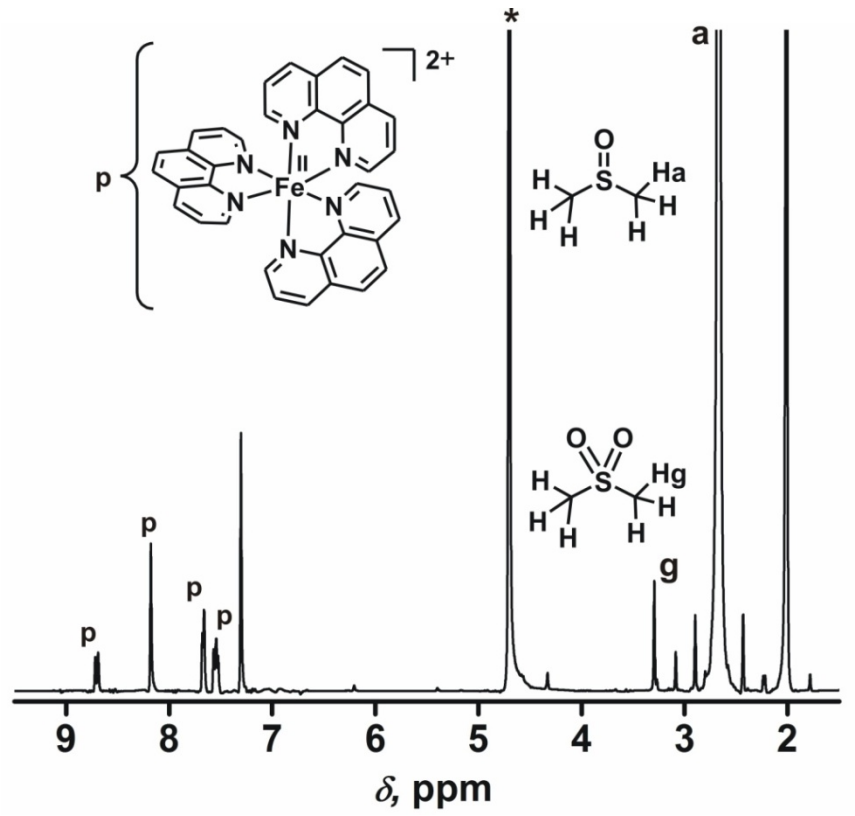

Fig. S21 ^{1}H NMR spectrum (500 MHz, D_2O, 295 K) of dimethyl sulfone formed in the reaction of **1** with O_2 in the presence of 10 eqv of dimethyl sulfoxide in acetonitrile. Peaks assigned with p are from tris(1,10-phenanthroline)iron(II) complex. Peak assigned with asterisk (*) is from residual solvent.

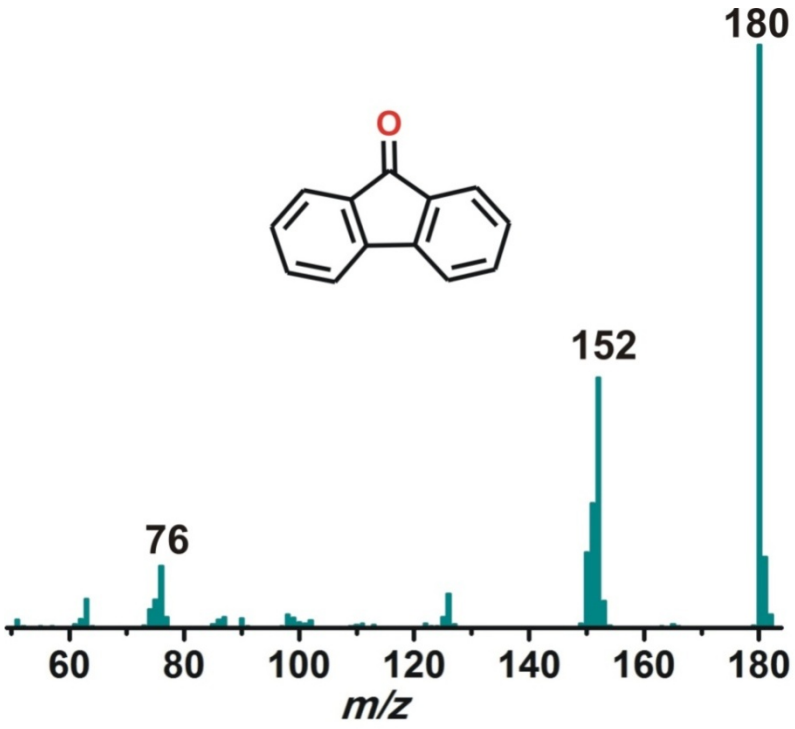

Fig. S22 GC-mass spectrum showing the formation of fluorenone in the reaction of **1** with fluorene in acetonitrile.

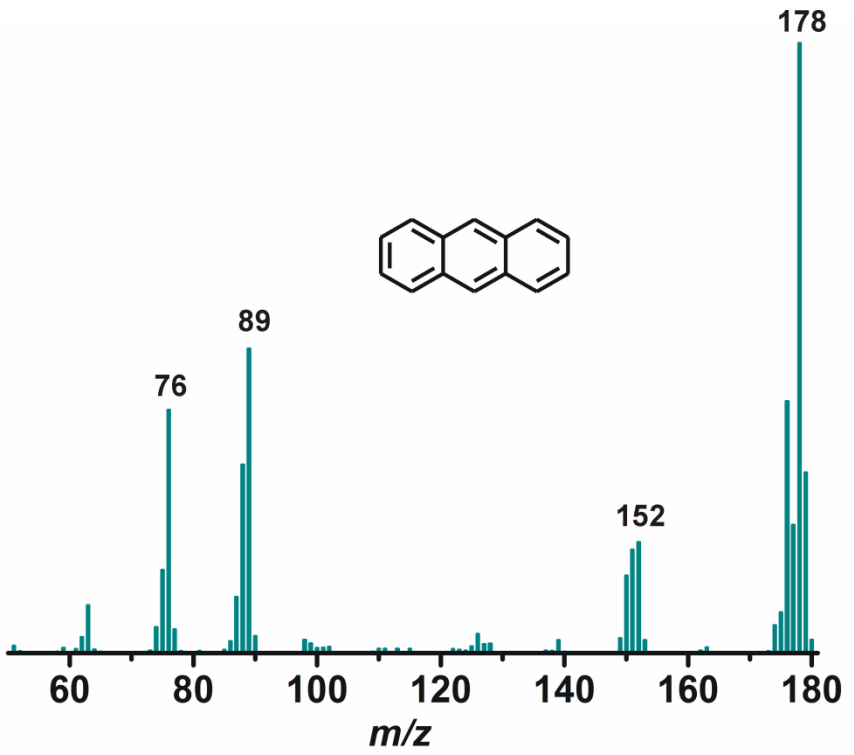

Fig. S23 GC-mass spectrum showing the formation of anthracene in the reaction of **1** with 9,10-dihydroanthracene in acetonitrile.

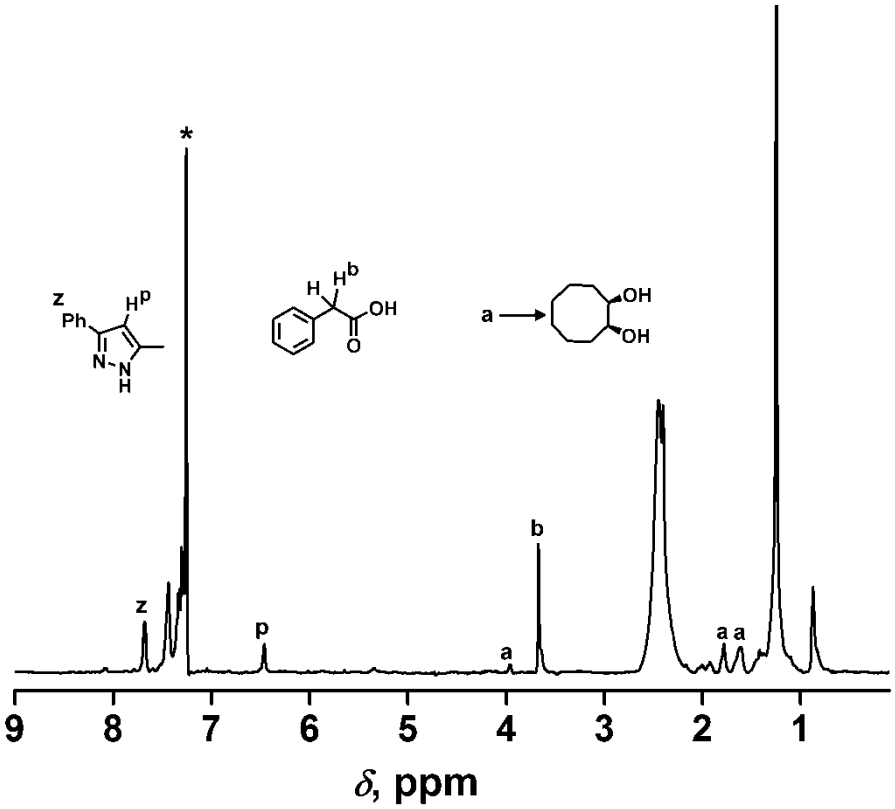

Fig. S24 ^{1}H NMR spectrum (500 MHz, $CDCl_3$, 295 K) of *cis*-cyclooctane-1,2-diol formed in the reaction of **1** with O_2 in the presence of 100 eqv of cyclooctene in acetonitrile.

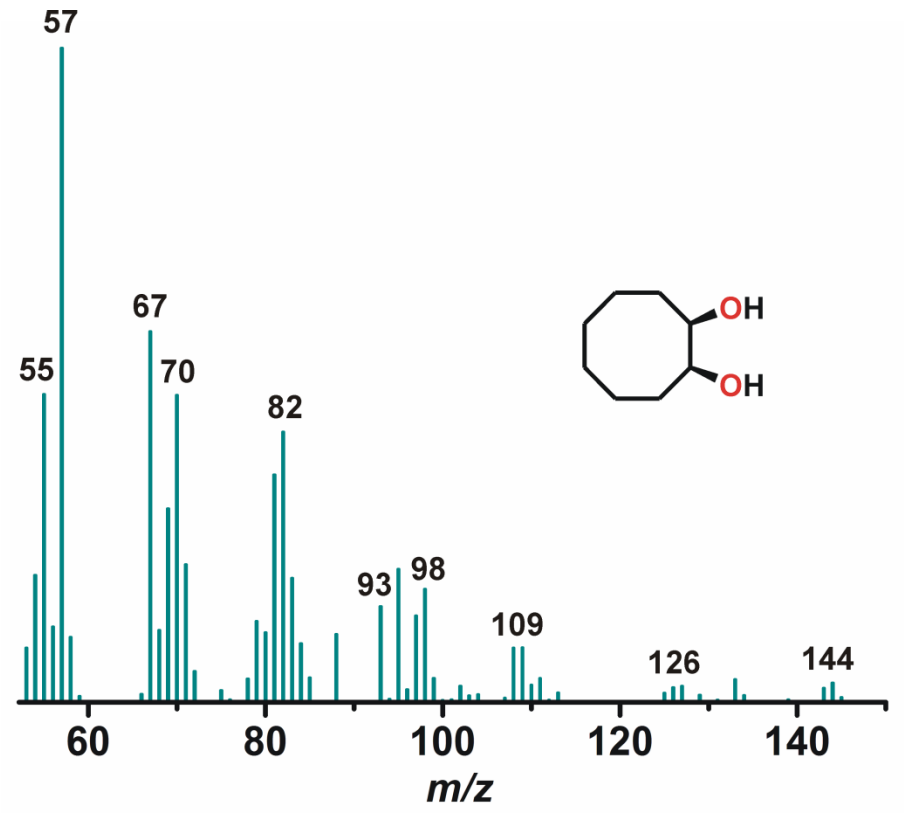

Fig. S25 GC-mass spectrum of *cis*-cyclooctane-1,2-diol formed in the reaction of **1** with cyclooctene.

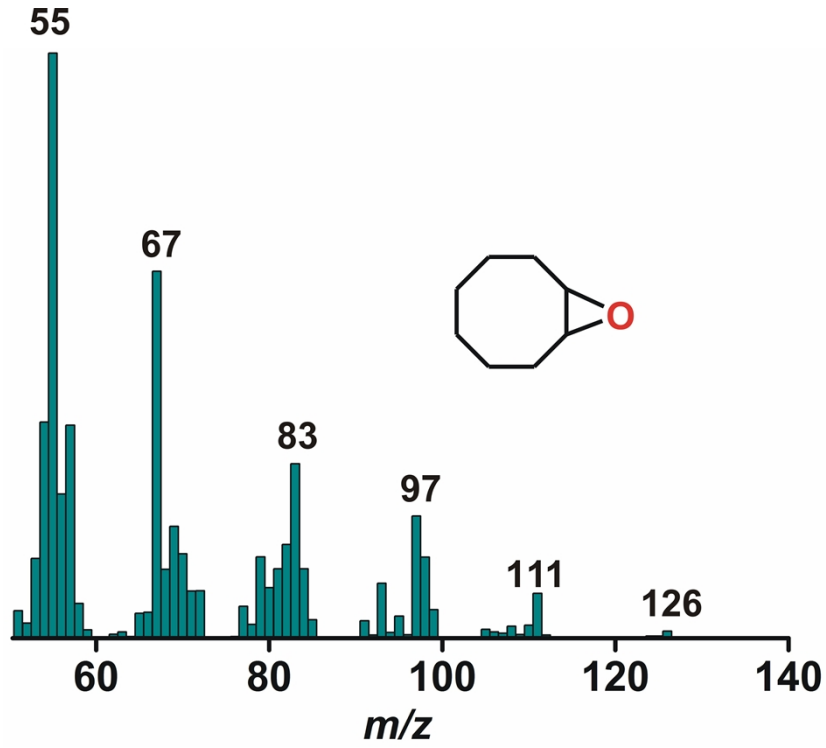

Fig. S26 GC-mass spectrum of cyclooctene oxide formed in the reaction of **1** with cyclooctene.

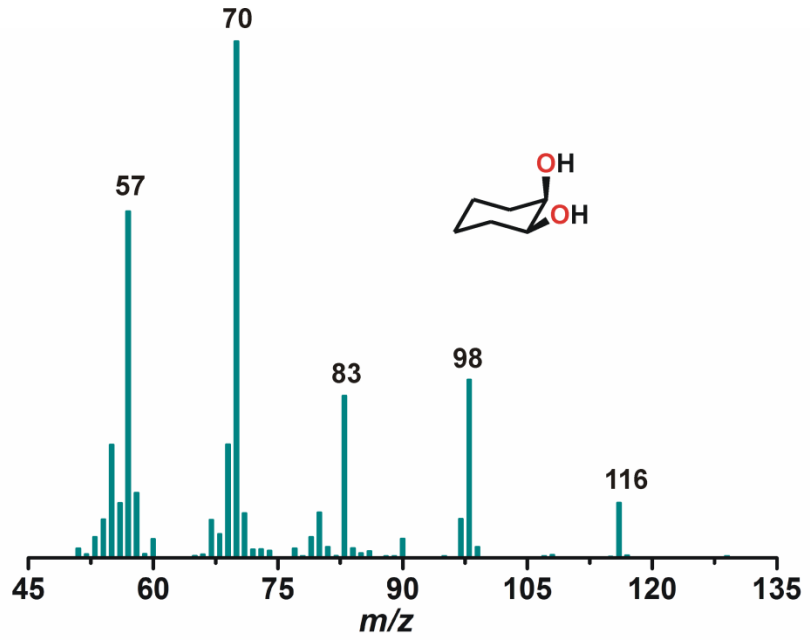

Fig. S27 GC-mass spectrum of *cis*-cyclohexane-1,2-diol formed in the reaction of **1** with cyclohexene.

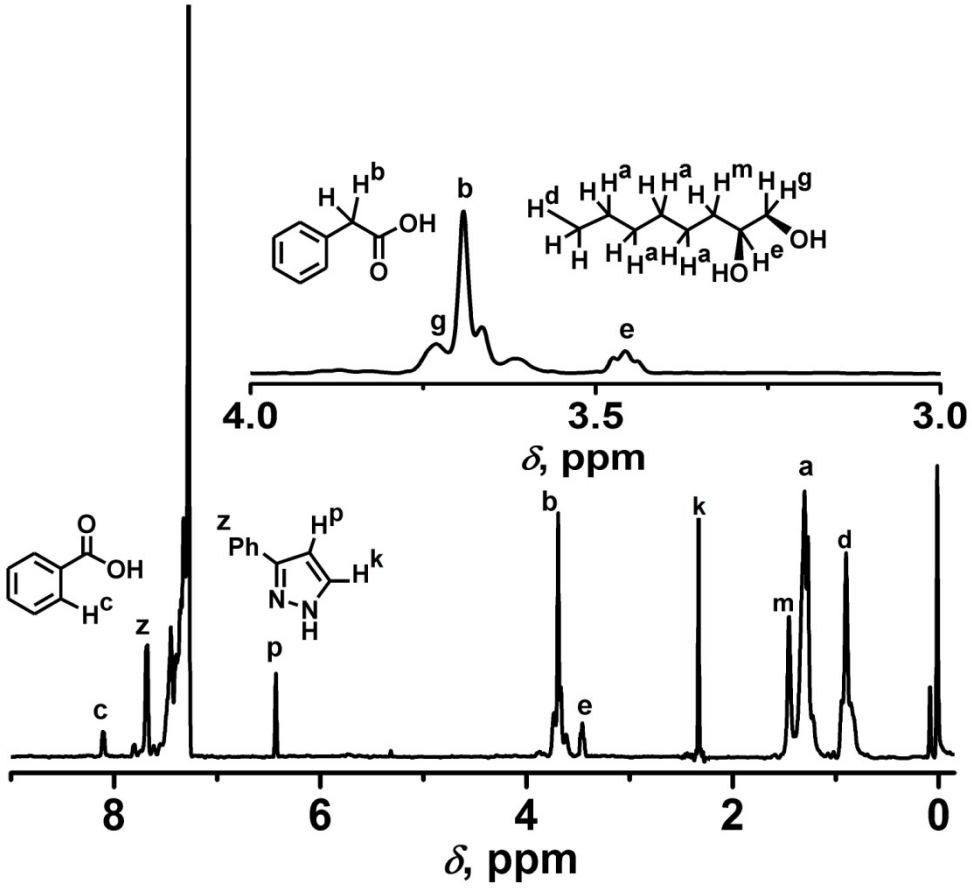

Fig. S28 ^{1}H NMR spectrum (500 MHz, $CDCl_3$, 295 K) of octane-1,2-diol formed in the reaction of **1** with O_2 in the presence of 100 eqv of 1-octene in acetonitrile.

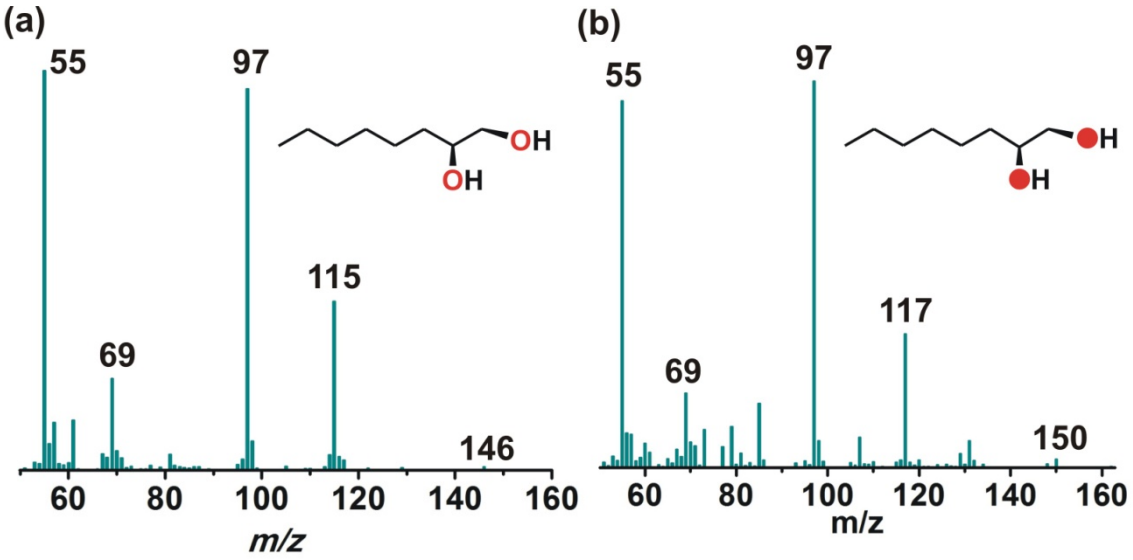

Fig. S29 GC-mass spectra of octane-1,2-diol obtained from 1-octene in the reaction of **1** with (a) $^{16}O_2$ and (b) $^{18}O_2$.

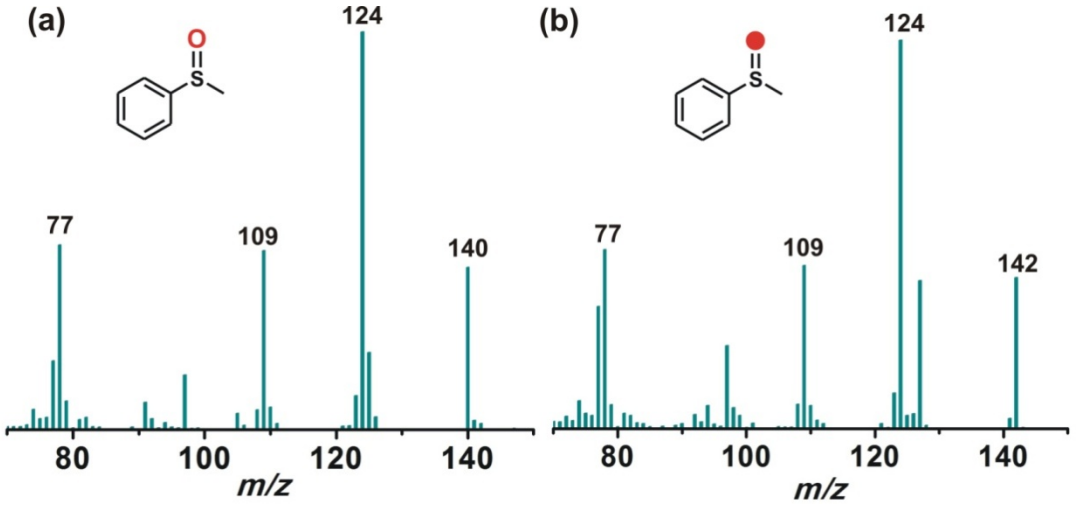

Fig. S30 GC-mass spectra of thioanisole oxide formed in the reaction of **1** with thioanisole in acetonitrile in the presence of (a) $^{16}O_2$ and (b) $^{18}O_2$.

References:

1. D. T. Puerta and S. M. Cohen, *Inorg. Chim. Acta*, 2002, **337**, 459-462.
2. S. Trofimenko, *J. Am. Chem. Soc.*, 1967, **89**, 6288-6294.
3. APEX 2 v2.1−0, Bruker AXS, Madison, WI, 2006.
4. Sheldrick, G. M. *SHELXL97, Program for Crystal Structure Analysis (Release 97-2)*; University of Göttingen: Göttingen, Germany, 1998.